

2001

Electron Heating in Atmospheric Pressure Glow Discharges

Robert H. Stark
Old Dominion University

Karl H. Schoenbach
Old Dominion University, kschoenb@odu.edu

Follow this and additional works at: https://digitalcommons.odu.edu/bioelectrics_pubs

 Part of the [Atomic, Molecular and Optical Physics Commons](#), and the [Plasma and Beam Physics Commons](#)

Repository Citation

Stark, Robert H. and Schoenbach, Karl H., "Electron Heating in Atmospheric Pressure Glow Discharges" (2001). *Bioelectrics Publications*. 201.
https://digitalcommons.odu.edu/bioelectrics_pubs/201

Original Publication Citation

Stark, R. H., & Schoenbach, K. H. (2001). Electron heating in atmospheric pressure glow discharges. *Journal of Applied Physics*, 89(7), 3568-3572. doi:10.1063/1.1351546

Electron heating in atmospheric pressure glow discharges

Robert H. Stark and Karl H. Schoenbach^{a)}

Physical Electronics Research Institute, Old Dominion University, Norfolk, Virginia 23529

(Received 29 August 2000; accepted for publication 21 December 2000)

The application of nanosecond voltage pulses to weakly ionized atmospheric pressure plasmas allows heating the electrons without considerably increasing the gas temperature, provided that the duration of the pulses is less than the critical time for the development of glow-to-arc transitions. The shift in the electron energy distribution towards higher energies causes a temporary increase in the ionization rate, and consequently a strong rise in electron density. This increase in electron density is reflected in an increased decay time of the plasma after the pulse application. Experiments in atmospheric pressure air glow discharges with gas temperatures of approximately 2000 K have been performed to explore the electron heating effect. Measurements of the temporal development of the voltage across the discharge and the optical emission in the visible after applying a 10 ns high voltage pulse to a weakly ionized steady state plasma demonstrated increasing plasma decay times from tens of nanoseconds to microseconds when the pulsed electric field was raised from 10 to 40 kV/cm. Temporally resolved photographs of the discharge have shown that the plasma column expands during this process. The nonlinear electron heating effect can be used to reduce the power consumption in a repetitively operated air plasma considerably compared to a dc plasma operation. Besides allowing power reduction, pulsed electron heating also has the potential to enhance plasma processes, which require elevated electron energies, such as excimer generation for ultraviolet lamps. © 2001 American Institute of Physics. [DOI: 10.1063/1.1351546]

INTRODUCTION

High pressure glow discharges are used in plasma processing, gas lasers, chemical and bacterial decontamination of gases, and as mirrors and absorbers of microwave radiation. The latter applications require the use of air plasmas at atmospheric pressure. Transient high pressure glow discharges in air, such as barrier discharges¹ and ac discharges,² are already well established but recently high pressure dc discharges with dimensions of centimeters have been generated by using novel plasma cathodes.^{3,4} One of them is a microhollow cathode discharge sustained plasma, where the microhollow cathode discharge provides the electrons for the main discharge. The elimination of the cathode fall, the cradle for glow-to-arc transition, has allowed us to generate dc glow discharges in atmospheric pressure air with electron densities of 10^{13} cm⁻³ and gas temperature below 2000 K.^{5,6} The electrical power density required to sustain these plasmas is approximately 5 kW/cm³, a power, which limits the size of the plasma to values on the order of cubic centimeter, due to economic and thermal management reasons.

The electric field strength required to sustain the 10^{13} cm⁻³ electron density plasma was measured as 1.2 kV/cm. At a gas temperature of 2000 K, the gas density N is 3.7×10^{18} cm⁻³, the reduced electric field strength E/N is consequently 32 Td. The electron energy distribution function $f(\varepsilon)$, where ε is the electron energy, in this case is fully determined by the reduced electric field E/N . For dry air (80% nitrogen+20% oxygen) at atmospheric pressure and an

E/N of 32 Td, $f(\varepsilon)$ is shown in Fig. 1. The electron energy distribution was calculated by means of ELENDIF.⁷ ELENDIF is a Boltzmann solver, which allows us to compute the electron energy distribution, the drift velocity, diffusion coefficient, energy flow rates, and rate coefficient for various processes in a homogeneous, partially ionized gas with time varying electric field applied. Processes considered with this code were excitation (rotational, vibrational, electronic), ionization (including the distribution of secondaries), recombination, and attachment. In addition electron-electron and electron-ion collisions were included.⁷

Also shown in Fig. 1, is the nonequilibrium electron energy distribution (for the case of a 1 ns rise time pulse of 120 Td amplitude after a time of 50 ns). It is clearly shifted into the range of increasing ionization cross sections, which are shown in the same figure for oxygen and nitrogen.⁸ The consequent increase in ionization rate leads to a strong increase in electron density. The electrons transfer their energy to the heavy particles, heating the gas. Gas heating leads to glow-to-arc transitions.³

In order to shift the electron energy distribution to higher energies, by means of a pulsed electric field, the duration of the pulse consequently needs to be less than the time for the development of these glow-to-arc transitions, which for atmospheric pressure glow discharges is on the order of 10 ns. The higher the electric field, the shorter the pulse needs to be. The increased rate of ionization causes a strong increase in electron density, as noted before. The increase in electron density from an initial value of 10^{13} cm⁻³, obtained by applying a 10 ns trapezoidal pulse with a rise and fall time of 1 ns right at the end of the pulse, is shown in Fig. 2 with the

^{a)} Author to whom correspondence should be addressed; electronic mail: schoenbach@ece.odu.edu

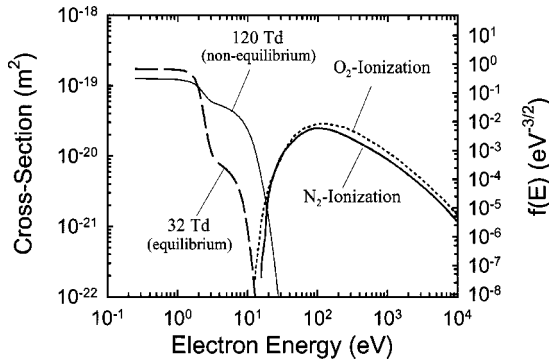


FIG. 1. Ionization cross sections of nitrogen and oxygen (Ref. 8), and the steady-state and transient electron energy distribution function (dashed and solid lines, respectively) for electrons in an atmospheric pressure air discharge. The steady state electron energy distribution function holds for an reduced electric field of $E/N=32$ Td. The solid line represents the nonequilibrium electron energy distribution obtained by applying a pulse with a rise time of 1 ns and an amplitude of 120 Td, at a time of 50 ns.

reduced electric field E/N as the variable parameter. As shown, with increasing E/N the electron density increases from values close to $1 \times 10^{13} \text{ cm}^{-3}$ (the assumed initial electron concentration) at 60 Td and below to $1.6 \times 10^{18} \text{ cm}^{-3}$ at 275 Td. Consequently, assuming that the electron losses after the E -field application are due to recombination only, the decay time of the electron density τ_d increases from tens of nanoseconds to microseconds. The decay time in this case is defined as the time it takes to reduce the electron density from its peak value n_p to an equilibrium value n_0

$$\tau_d = \frac{(n_p - n_0)}{(\beta n_0 n_p)}, \quad (1)$$

with β being the electron-ion recombination coefficient. This time, τ_d approaches the constant value

$$\tau_d = \frac{1}{\beta n_0} \quad (2)$$

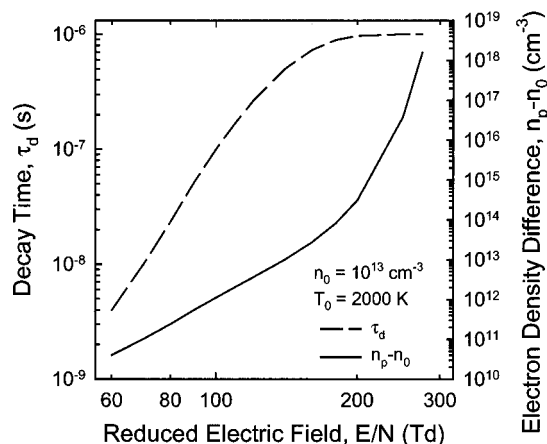


FIG. 2. Electron density difference $n_p - n_0$ (solid line) and decay time due to recombination (dashed line) vs amplitude of the 10 ns applied electric field pulse. The decay time is defined as the time it takes for the plasma to reach the initial electron density, in this case 10^{13} cm^{-3} .

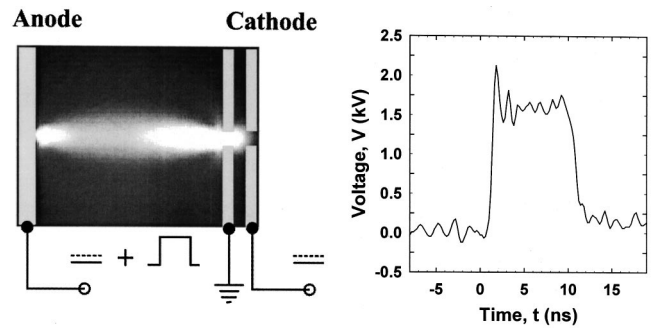


FIG. 3. Experimental setup and temporal development of the 10 ns high voltage pulse ($V_{\text{pulse}} = 1.6 \text{ kV}$). The microhollow cathode discharge and the MHCD sustained glow are operated in a direct current mode ($I = 10 \text{ mA}$). A 10 ns high voltage pulse of variable amplitude is applied at the anode, superimposed to the dc voltage.

for $n_p \gg n_0$. For air with an assumed $\beta \approx 10^{-7} \text{ cm}^3/\text{s}$ (Ref. 9) and an equilibrium electron density of 10^{13} cm^{-3} it is on the order of $1 \mu\text{s}$.

In order to explore the electron heating effect of short electric pulses in a high pressure gas we have studied the temporal decay of the electron density in a microhollow cathode discharge (MHCD) sustained plasma in atmospheric pressure air. The temporal development of electron density after applying a short electric pulse is reflected in the temporal development of the electrical parameters of the discharge and the emission of recombination radiation. Both quantities were measured dependent on the amplitude of the applied 10 ns pulse. In addition the temporal development of the discharge plasma was recorded by means of a high speed camera.

EXPERIMENTAL SETUP

A schematic sketch of the experimental setup is shown in Fig. 3. The MHCD serves as the plasma cathode, which sustains a stable atmospheric pressure glow discharge.⁴ The MHCD plasma is generated between two plane-parallel molybdenum electrodes, which are separated by an alumina spacer $100 \mu\text{m}$ in thickness. Electrode distance and diameter of the circular opening in the center of the electrodes are $100 \mu\text{m}$, respectively. The glow discharge, sustained by the MHCD plasma cathode fills the gap between the plasma cathode and a positively biased, third electrode at a distance of 1 mm . Both plasma cathode and the supported glow discharge were operated by dc in atmospheric humid air at 10 mA discharge current. Inserted into the electrode schematics in Fig. 3 is a side-on photograph of the air glow. The diameter of the plasma column is typically $800 \mu\text{m}$. In order to shift the electron energy distribution function to higher energies a 10 ns, high voltage pulse was superimposed on to the dc glow. Shown in Fig. 3 is the measured pulse shape of the high voltage pulse. Rise time and fall time of the trapezoidal pulse is approximately 1 ns.

The high voltage pulse is generated by a pulse forming network (PFN) in strip-line geometry. Figure 4 shows the schematics of the 10 ns pulse generator. The PFN consists of two metal strips separated by a dielectric. The strip-line has an impedance of 10Ω . The electrical energy is switched into

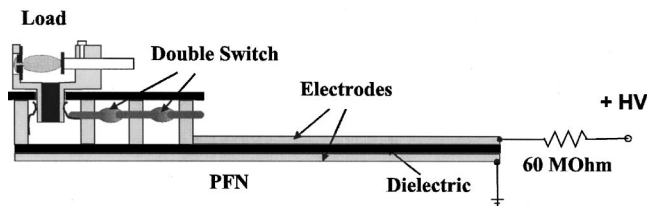


FIG. 4. Schematics of the $10\ \Omega$ strip-line pulse generator. The second switch in the double switch arrangement served as pulse sharpener (reduction of rise time).

the load by means of a pressurized spark gap with nanosecond pulse rise time. The pulse generator is operated in self-breakdown mode at “single shot” conditions.

The discharge current and the voltage across the pulsed glow discharge have been monitored by means of fast rise time, high voltage probes (Tektronix, 350 MHz) and a 400 MHz digitizing oscilloscope (Tektronix TDS 380). In addition, measurements of transient emission of plasma radiation in the visible have been performed. The optical emission from the center of the glow discharge gap was observed side-on by means of a photomultiplier tube (PMT) (Hamamatsu R1533) with a sensitivity range between 300 and 650 nm. The PMT measurements were complemented by high-speed photography. A high-speed camera (ICCD Max, Stanford Research Institute) was used to study the development of the glow discharge plasma column temporally and spatially resolved. The camera was triggered by the signal of the voltage monitor of the 10 ns pulse generator. The internal delay of the camera, which is approximately 80 ns, limited the study of the plasma to the afterglow phase of the discharge. The camera is equipped with an image intensifier (microchannel plate) and allows measurements with a temporal resolution up to 2 ns. However, due to the relatively low level of light emitted by the plasma, the exposure time was set to 200 ns.

RESULTS

Figure 5 shows the temporal development of the voltage across the glow discharge plasma in response to high voltage pulses of various amplitudes (superimposed to the dc volt-

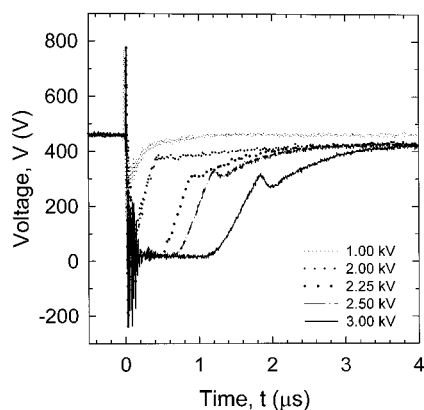


FIG. 5. Response of the plasma to the high voltage pulse: voltage across the glow discharge vs time for various pulse voltages (gap distance=1 mm).

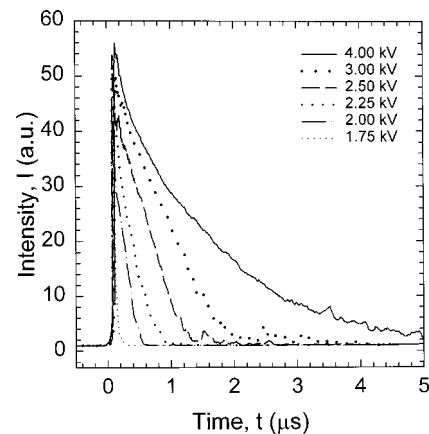


FIG. 6. Temporal development of the optical emission in the visible and near ultraviolet after pulse application. Parameter is the electrical pulse amplitude (gap distance=1 mm).

ages). The voltage across the dc plasma decreases within a few nanoseconds after application of the pulsed voltage by 1 order of magnitude. The sustaining electric field drops to values as low as 300 V/cm for an applied pulse with 20 kV/cm amplitude. Depending on pulse amplitude the discharge electric field remains at this low level for several hundred nanoseconds for 10 kV/cm pulses, up to 1.8 microseconds for 30 kV/cm pulses. During recovery of the discharge voltage, at approximately 3 kV/cm, a dip in voltage is observed. This dip may be caused by interaction of the glow discharge with the sustaining plasma cathode, which turns on again at this voltage, after seemingly not being active from the time of applied pulse to this point in time. After this dip, the rise of the voltage slows by more than a factor of 2.

Figure 6 shows the temporal development of the optical emission of the plasma in the visible and near ultraviolet in response to the 10 ns voltage pulse for various pulse voltages. When the high voltage pulse is applied, the intensity rises within nanoseconds by almost 2 orders of magnitude over the dc value. The peak intensity varies only slightly with pulse voltage. After pulsing the intensity decays to the dc level on a time scale which is several orders in magnitude larger than the duration of the applied pulse.

Figure 7 shows the increase in decay time with increasing pulsed electric field amplitudes, evaluated from electrical and optical measurements (Figs. 5 and 6). The decay time increases nearly linearly with pulsed electric field from 165 ns at 17.5 kV/cm to $3.6\ \mu\text{s}$ at 40 kV/cm. For the optical measurements the decay time has been defined as the time the intensity decays to 10% of the maximum value, for the electrical measurements as increase in voltage from the lowest sustaining voltage to 300 V, a value which corresponds to approximately 70% of the dc value. The reason for the choice of these definitions is discussed in the following section.

High-speed photography in the afterglow of the plasma shows the formation of a luminous plasma close to the anode. The optical emission of the pulsed plasma was such that even for an exposure time of 200 ns, the remaining parts of

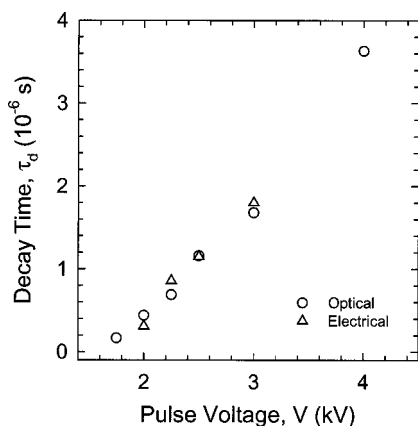


FIG. 7. Decay time vs pulsed electric field, obtained from the electrical and optical measurements (see also Fig. 5 and 6).

the plasma between anode and cathode could not be observed. The diameter of the plasma at the anode is up to 5–10 times the diameter of the dc plasma column (Fig. 3). It decays on a time scale of microseconds, in accordance with electrical and PMT measurements (Figs. 5 and 6).

DISCUSSION

Although the results of the measurements are not comprehensive (e.g., in order to obtain the electron density from electrical measurements, we would need to know the values of the local electric fields and the current density in addition to the electron mobility), certain conclusions on the effect of electrical pulses on the physics of the discharge and on the temporal development of the electron density can be drawn. When the high voltage pulse is applied, the current changes rapidly, and the microhollow cathode discharge is no longer able to provide the required electrons to sustain the discharge. The current in this phase consists of conduction current plus displacement current. The displacement current is estimated to be on the order of 1 A. Higher currents can only be conduction currents, most likely generated by extending the cathode surface; this means by generating a discharge, which at least for a short time is sustained by secondary electron processes at the cathode, rather than by the MHCD. This hypothesis is supported by the high speed photographs, which show an expanded plasma channel after pulse application. With reduced conductivity (increasing voltage across the gap) the plasma cathode eventually takes over again. This might explain the dip in the recovering voltage seen in Fig. 5, and the subsequent change in slope.

The electron decay time increases linearly with the amplitude of the applied electric field pulse. This is shown in Fig. 7, where the time for voltage recovery, defined as the time where the voltage reaches 70% of its dc value (corresponding to a decrease in conductivity to 30% of its maximum value), is plotted versus the applied electric field. Since the conductivity is proportional to the electron density, this curve provides us with information on the electron decay time, assuming that the current density remains constant. Also shown in this graph is the decay time of the optical emission, defined as the time where the intensity has decayed

to 10% of its initial value. Assuming that the decay of the electron density is due mainly to recombination, the optical emission varies with the square of the electron density. A decay of the intensity to 10% would consequently correspond to a decay of the conductivity to 30%. The experimental results, obtained from electrical and optical measurements, agree well and also agree reasonably well with theoretical results (Fig. 2), considering the uncertainty in the value of the recombination coefficient β .

One of the incentives for this study was to explore the pulsed electron heating effect as a means of reducing the power consumption of atmospheric pressure glow discharges in air. For this application a pulsed electric field would be applied repetitively to a base plasma with a low degree of ionization. This electrical pulse, if shorter than the time for the development of glow-to-arc transitions, would raise the electron density to values n_p exceeding the desired electron density n_0 for a particular application. The electron density would then decay. When it reaches a certain value below n_0 a second pulse would be applied to bring the density up to n_p again. This process, which would generate a plasma with an average electron density of n_0 , could be repeated *ad infinitum*.

Experimental studies with the same pulse generator (but applied to a differently sustained dc plasma than the one described in this article) and modeling studies have shown that for the 10 ns pulse, this mode of operation allows us to create a plasma with an average electron density of n_0 at a fraction of the energy cost that is required to generate the same electron density in a dc plasma.¹⁰ In these experiments the background gas temperature was kept constant over an area of about 1 cm in diameter, large compared to the diameter of the discharge plasma column, using a plasma torch. A two pin electrode configuration has been used to generate an atmospheric pressure dc plasma, which was then superimposed by the 10 ns high voltage pulse. It could be shown that it is possible, using this pulsed electric field method, to reduce the power consumption in an atmospheric pressure air plasma with an n_0 of $2.8 \times 10^{12} \text{ cm}^{-3}$ by a factor of 150 compared to the dc case.¹⁰

Is it possible to reduce the power even more by reducing the pulse duration further? Results of ELENDF calculations are shown in Fig. 8 for pulses with duration ranging from 3.8 to 20 ns. The lower limit in pulse duration is determined by the present status of the pulsed power technology. Although there are now pulse generators available which generate high voltage pulses with duration down to 300 ps,¹¹ the system costs rise for pulse generators with pulse widths below nanoseconds, possibly offsetting the power savings effect. The upper limit was chosen, because overvoltage pulses with duration much longer than 10 ns generally cause glow-to-arc transitions in atmospheric pressure air. The voltage pulses were assumed to have a 1 ns rise and fall time and a flat top.

Shown is the electric field intensity required to reach electron densities of $5 \times 10^{13} \text{ cm}^{-3}$, starting out with 10^{13} cm^{-3} , versus pulse duration. This electric field increases with reduced pulse duration. The average power, however, which is defined as the energy provided by the pulse to the plasma, divided by the time it takes for the electron density

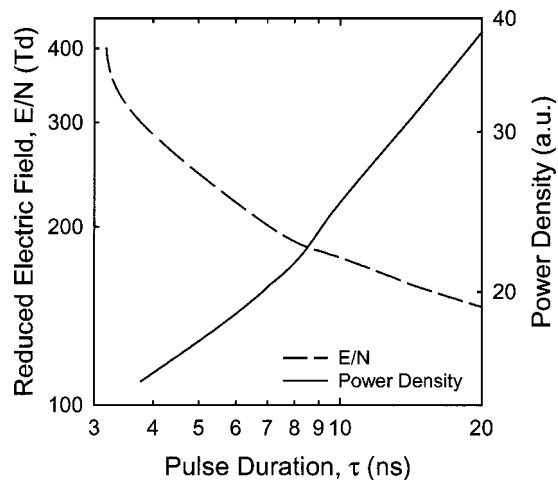


FIG. 8. Pulse duration and electric field amplitude, required to increase the electron density from the dc value ($n_0=10^{13} \text{ cm}^{-3}$) to a peak value ($n_p=5 \times 10^{13} \text{ cm}^{-3}$), and corresponding electrical power density $(E/N)^2 \cdot \tau / \tau_d$, where τ is the pulse duration and τ_d is the decay time.

to relax to its base value, decreases with decreasing pulse duration. Reducing the pulse duration by a factor of 3 from 10 to 3.5 ns promises to provide additional power savings over the 10 ns pulse by a factor of 2. This would reduce the average power density for a 10^{13} cm^{-3} electron density atmospheric pressure air plasma by a factor of 300 from about 5 kW/cm^{-3} to 16 W/cm^{-3} .

Besides the use in power reduction as demonstrated in this article, a promising application of the pulsed electric field method is the use in plasma chemistry. By applying short pulses of high electric fields, the electron energy distribution function can be shifted temporarily to high electron energies. By choosing the right electric field strength and

consequently the right pulse duration, this technology has the potential to selectively activate and control certain plasma chemical processes,¹² which in other types of glow discharges have a low efficiency. Such applications are: plasma processing, e.g., the generation of radicals in plasmas for destruction of volatile organic compounds, and the generation of excimers in excimer lamps and excimer lasers.

ACKNOWLEDGMENT

This work was supported by the Air Force Office for Scientific Research (AFOSR) in cooperation with the DDR&E air plasma ramparts MURI program.

- ¹B. Eliasson and U. Kogelschatz, *IEEE Trans. Plasma Sci.* **19**, 309 (1991).
- ²S. Kanazawa, M. Kogoma, T. Moriwaki, and S. J. Okazaki, *J. Phys. D* **21**, 836 (1988).
- ³E. Kunhardt, *IEEE Trans. Plasma Sci.* **28**, 189 (2000).
- ⁴R. H. Stark and K. H. Schoenbach, *Appl. Phys. Lett.* **74**, 3770 (1999).
- ⁵R. H. Stark, U. Ernst, M. El-Bandrawy, C. Laux, and K. H. Schoenbach, 30th AIAA Plasmadynamics and Lasers Conference, Norfolk, VA, July 1999, paper AIAA-99-3666.
- ⁶F. Leipold, R. H. Stark, A. El-Habachi, and K. H. Schoenbach, *J. Phys. D* **33**, 2268 (2000).
- ⁷W. L. Morgan and B. M. Penetrante, *Comput. Phys. Commun.* **58**, 127 (1990).
- ⁸A. V. Phelps, in *Gaseous Dielectrics V*, edited by L. G. Christophorou and D. W. Bouldin, (Pergamon, New York, 1987), p. 1.
- ⁹Y. P. Raizer, *Gas Discharge Physics* (Springer, Berlin, 1991), p. 60.
- ¹⁰M. Nagulapally, G. V. Candler, C. O. Laux, L. Yu, D. Packan, C. H. Kruger, R. H. Stark, and K. H. Schoenbach, 31st AIAA Plasmadynamics and Lasers Conference, Denver, VA, July 2000, paper AIAA 2000-2417.
- ¹¹V. M. Efanov, A. V. Kriklenko, P. M. Yarin, and N. I. Daviduk, *Conference Record, 24th International Power Modulator Symposium*, Norfolk, VA, June 2000, p. 201.
- ¹²H. Sugawara, T. Shimoda, and Y. Sakai, *Proceedings International Symposium Electron-Molecule Collisions and Swarms*, Tokyo, Japan, 18–20 July 1999.